

A new histogram quantization algorithm for land cover mapping

Josef Cihlar¹, Galina Okouneva², Jean Beaubien³, and Rasim Latifovic²

- 1) Canada Centre for Remote Sensing, Ottawa, Ontario
- 2) Intermap Technologies, Ottawa, Ontario
- 3) Canadian Forest Service, Quebec City, Quebec

Corresponding author: J. Cihlar, tel 613 947 1265; fax 613 947 1406; email josef.cihlar@ccrs.nrcan.gc.ca

Abstract

Land cover mapping from multispectral satellite data is based primarily on spectral differences in land cover categories. Since only a limited number of cover types are desired in most cases, the images contain redundant information which unnecessarily complicates the digital mapping process. In this study, we have devised an algorithm to automatically and reproducibly quantize an image to be classified into a reduced number of digital levels, in most cases without a visually perceptible reduction in the image information content. The Flexible Histogram Quantization (FHQ) algorithm assumes that the histogram has one or two major peaks (representing water and/or land) and that most of the information of interest is in one peak. It aims to provide a sufficient quantization in the main peak of interest as well as in the tails of this peak by computing an optimized number of quantized levels and then identifying the range of digital values belonging to each level. A comparison of the FHQ with four existing quantization algorithms showed that the FHQ retained substantially more radiometric discrimination than histogram normalization, linear quantization, and scaling methods. Using a random sample of Landsat TM images and an AVHRR coverage of Canada, the average quantization error for the FHQ was 1.68 digital levels for an entire scene and 1.41 for land pixels only. Based on the 34 single-band test images included in the comparison, the radiometric resolution was reduced from 255 to 23.3 levels on the average, or by a factor of 10.94ⁿ for a multispectral image with n spectral bands. Compared to the other quantization methods, FHQ had a higher efficiency (by 65% to 148%), except for histogram equalization. FHQ also retained more information than histogram equalization (by 11%) but more importantly, it provided finer resolution in the tails of the main histogram peak (by 36 - 664%, depending on the position in the tails) for infrequent but potentially important land cover types. In addition, unlike the other methods the FHQ does not require a user-specified number of levels and therefore its results are fully reproducible. The FHQ can be used with single scenes, with radiometrically seamless mosaics, or when classifying radiometrically incompatible adjacent scenes. It is concluded that the FHQ provides an effective means for image quantization, as an automated pre-processing step in land cover mapping applications.

Introduction and objectives

In simple terms, the objective of land cover mapping is to divide the territory of interest into discrete homogenous parcels of land, or polygons, and then to assign a name to each parcel from a list of eligible names, i.e. the mapping legend. Earth observation (EO) data and their ability to provide spectral information are often used in this process. It is recognized that there is not always a 1:1 correspondence between land cover of a desired mapping legend and the information content of the EO data. This is because some of the classes of interest may not have unique spectral expression, or because of the imperfections in the information extraction process. Fundamentally, nothing can be done in the analysis to remove the former deficiency; instead, it is necessary to change the mapping legend or choose another approach to obtaining the desired land cover information. On the other hand, much can be done to remedy the second problem since in principle, the analyst has full control over the information extraction process.

In practice, the best one can hope for is to extract all relevant land cover-related information from the EO image data and then translate it into the mapping legend employed. A variety of approaches have been developed for this purpose (e.g., Mather, 1987). ‘All relevant’ implies that some information inherent in the EO data is redundant for land cover mapping purposes, specifically that which describes variations within cover types. Indeed, even in 8-bit data and with few spectral channels there are many more possible spectral combinations than could be retained as distinct land cover types, since most mapping legends have only a few dozen classes at best.

The reduction of the within-parcel spectral differentiation is a key part of land cover mapping by visual interpretation (e.g., Rabben, 1960). The interpreter focuses on the sharp discontinuities between parcels while mentally smoothing out differences within the land parcels. However, reduction in the number of digital levels can also be a very effective step in digital classification because it reduces the possible number of classes that can be identified subsequently. The effectiveness of the reduction in the radiometric resolution of spectral data, i.e. histogram quantization, has been demonstrated in digital classification algorithms (Beaubien, 1994, Beaubien and Simard, 1993). Beaubien (1994) and Beaubien et al. (1997) also described how the quantization can be optimized by an analyst. Unfortunately, such results are difficult to reproduce by others, thus leading to inconsistencies in applications over larger areas, by other mapping teams, or over time. The challenge is in devising an objective approach to quantization which retains the relevant land cover information. The objective of this paper is to describe such an algorithm and to test its performance.

Rationale and algorithm

Rationale

Ideally, an image quantization algorithm for land cover mapping should meet several criteria:

1. Retain all the information which is needed to delineate individual land cover types recognized by the mapping legend employed (typically a few to several dozen classes).
2. Be sensitive to the information content of the scene, including the presence of important classes with a small number of pixels.
3. Select an optimum number of digital levels. 'Optimum' means selecting as few levels as possible without losing important land cover information. This is required to simplify the classification process by excluding unnecessary information from the quantized data.
4. Be easily reproducible by various investigators, including resistance to analyst bias; ideally be automated and not require user input.

A variety of image quantization algorithms which meet some of these criteria have been developed and are available in most commercial packages (e.g., Mather, 1987; PCI, 1997). For example, the often-used histogram equalization method (Jensen, 1996) is scene-sensitive in that it divides the full histogram into segments containing nominally equal fractions of the total number of pixels. However, this causes the quantization levels near the peak to be much narrower than those in the wings of the histogram, thus emphasizing land cover types typical for the scene and losing information on less well represented (but potentially important) cover types. In the linear quantization method (Jensen, 1996) the width of the digital levels is constant. If the quantization width is small enough, the important information will be retained across the histogram but at the expense of efficiency because only a small fraction of the pixels usually resides outside the main histogram peak. These few pixels then consume disproportionately high amounts of the computing and analysis effort. In the case of histogram normalization (Mather, 1987), the quantization is based on fitting the original histogram to a normal distribution, and the result will depend on the departure of the original histogram from the Gaussian curve.

The above methods have other disadvantages. In all cases, the analyst must define the number of levels. Unless based on preliminary tests, such a decision tends to be arbitrary and not reproducible by other investigators. Also, the algorithms are applied to the whole scene and thus do not differentiate between land and water, yet the detailed spectral information is only important for land.

In mapping studies using Landsat Thematic Mapper (TM) data, Beaubien (1994) described an interactive approach which optimizes the information content of the quantized images for land cover mapping in the boreal environment. It consists of several steps:

- Identify extreme-brightness land cover types in each spectral band. In boreal environments, these are (dark, followed by bright target) water and bare soil/rock in TM band 3; water and broadleaf forest in TM band 4; and water and bare soil/rock in TM band 5.
- Identify representative samples of these cover types and their typical digital levels. Thus, clouds and other unwanted categories are ignored.
- Expand the portion of each histogram between the two extreme targets to the entire range of values (e.g., 256 levels for TM).
- Perform linear quantization of each contrast-stretched histogram to 11 levels. These values were found through trials as the number of levels at which minimal difference could be visually perceived between the stretched image (step 3) and the quantized image.

This approach meets the criteria 1-3 above for an optimal quantization and has been proven effective for land cover mapping from TM and AVHRR data in boreal environments (north of 45°; Beaubien, 1994; Beaubien and Simard, 1993; Beaubien et al., 1997). It is efficient, scene-sensitive, and retains land cover information that permits the differentiation of the individual land parcels. It also performs a degree of normalization between multiple scenes because the extreme-brightness targets are assigned to the same digital levels in the quantized data. On the other hand, because of the reliance on the identification of representative reference targets in a scene it is difficult to reproduce. In this paper, we have used some features of the above approach as part of a new automated quantization algorithm based on the shape of the image histogram.

Flexible Histogram Quantization (FHQ) Algorithm

Consider a simple histogram of a scene dominated by land surface. Conceptually, its histogram consists of three regions (Figure 1): Region A - the main (or 'land') peak in which most of the pixels are located, representing the dominant cover types and thus requiring sufficient radiometric resolution so that no significant land cover type information is lost; Region B - the tails of the histogram representing infrequent cover types which nevertheless still require adequate resolution; and Region C - the remaining parts of the histogram which contain no land cover information of interest (water, clouds) or very rare cover types or conditions. The radiometric resolution of the quantized image should thus be highest for Region A and lowest for Region C. Histogram equalization provides this but it has poor balance between the widths of the levels in the peak (too narrow) and the wings (too wide).

Since no specific cover types can be selected automatically (such as in Beaubien's methodology where is achieved through visual interpretation and an analysis of digital values) we have chosen to consider Region A to be the histogram portion inside the inflection points of the main peak. Beyond the inflection points (Region B) the digital levels should broaden somewhat; the change

should be gradual until the portion with few pixels (Region C) is reached on each side of the histogram peak. This poses the following questions:

1. How many levels should there be in Region A?
2. How should the width change outside Region A?

Regarding the first question, a simple approach might be to use a fixed number of levels. However, this approach may not be efficient for histograms with narrow central peaks where the wings (Region B) may contain a significant portion of the pixels. The number of levels inside Region B should thus depend on the fraction of pixels present in Region A. To find a suitable formulation we selected representative shapes from among 120 histograms of growing season images across Canada (40 scenes, TM bands 3, 4, 5). After examining the shapes of these histograms we have selected the following formula:

$$DNL = a - \frac{b}{f}, \quad [1a]$$

where DNL = the number of quantized levels between the inflection points of the main histogram peak (i.e., Region A);

a, b = coefficients (dimensionless);

f = the fraction of pixels between the inflection points of the main histogram peak relative to all pixels in the image ($f \leq 1$, dimensionless).

Figure 2 shows the differences in DNL as a function of f for various combinations of a and b. In the histograms we examined (examples in Figure 4) f ranged from 0.55 to 0.82. Since in this range the a=20, b=5 combination yields the highest number of levels (Figure 2) we have chosen it for subsequent work. In this case the DNL values range from 11 to 14, well within the range found by Beaubien (1994). The DNL from Eq.[1a] is a 'safe' value since the inflection points lie inside the range of interest and the total number of levels will thus be higher than the target value of 11. Below $f=0.5$ the curve defined by Eq.[1a] decreases rapidly. Therefore, taking $f=DNL=0$ and $f=0.5$, $DNL=10$ as the limiting values DNL can be computed in this range as:

$$DNL = 20 * f. \quad [1b]$$

Since values $f < 0.5$ were not encountered in this data set we could not test the appropriateness of Eq.[1b] (see also Comments).

The width of the quantized levels QW inside Region A will be:

$$QW = \frac{I_{\max} - I_{\min}}{DNL}, \quad [2]$$

where I_{\max} (I_{\min}) is the digital level of the higher (lower) inflection point of the main peak.

As noted above QW should increase outside the inflection points but not too rapidly. This can be achieved by making the increase dependent on the change in the number of pixels. For the right-hand wing of the histogram, this takes the form:

$$QW(i) = \frac{c * QW(i-1) + d * EQW(i)}{c + d}, \quad [3]$$

where:

EQW= equivalent quantized level width, i.e. one for which the number of pixels would be the same as for the level $i-1$;

i = quantized level identifier.

Note that the $i, i-1$ exchange positions on the left-hand side of the histogram peak.

Equation [3] makes the widening of the quantized levels depend partly on the width of the previous level and partly on the rate of change in the number of pixels. It can be seen that this is a flexible combination of two approaches, the histogram equalization ($c=0$) and linear quantization ($d=0$). We have experimented with $c=d=1$ and $c=1, d=2$ and found a typical difference of 1-2 quantized levels. Since the former ($c=d=1$) provides higher resolution in Region B of the histogram we have used it as the baseline.

Given a histogram of an image for one spectral band, Equations [1]-[3] determine the widths and the number of quantized levels for the image. To complete the quantization, these levels must be placed over the histogram. This is done by finding the peaks, minima and inflection points for the histogram; centring the first quantized level on the main peak of the histogram; and computing the limits for other quantized levels on both sides of the peak until the extreme values (0, 255 for an 8-bit image) are reached; that is, the lower (upper) limits of regions B or C are not determined explicitly. The steps in the algorithm are summarized in Figure 3. To make the process analyst-independent, the identification of the main points on the histogram (peaks, inflection points, minima) needs to be automated and the three formulas can then be readily applied.

Data and methods

A set of TM images was selected from among 40 archived Landsat TM data of Canada. Most of these were obtained from previous (mutually unrelated) studies across the country and can thus be considered a random sample, possibly biased by the interest in land cover issues in those studies. The histograms of bands 3, 4, and 5 selected from these images were printed and subjectively grouped into categories according to the histogram shape. Examples were then

selected from each category so that the various types of histograms are well represented. Four images of all Canada prepared from composites of the NOAA Advanced Very High Resolution Radiometer (AVHRR; channels 1,2, seasonal mean normalized difference vegetation index (NDVI), area under the NDVI curve) were also used (Cihlar et al., 1997). For each selected image/histogram (input gray levels 0-255 in all cases), five quantization algorithms were employed:

1. The Flexible Histogram Quantization (FHQ) algorithm described above. In addition to the exact quantized levels (i.e., the gray level values belonging to a given quantized level), the total number of quantized levels TNL was obtained and used as an input parameter in the other algorithms. To smooth the original histogram we used the Fast Fourier Transform method (Brigham, 1974). This method consists of three steps: transforming the data into the frequency domain, multiplying the resulting complex data by a smoothing (low pass) filter, and re-transforming the product back into the spatial domain to yield the smoothed histogram.

In the computer implementation, it was assumed that the histogram consists of two peaks separated by a local minimum. Smoothing of the original histogram was done using PVWAVE programming language (PVWAVE, 1993) and its function `fft` which was applied twice:

$$result = fft(fft(h,-1) * f,1), \quad [4]$$

where h is the original histogram and f is the filter. The values -1 and 1 specify the direction of the transformation: -1 into the frequency domain and 1 into the spatial domain. First, the original gray values histogram curve h is transformed into the frequency domain to obtain the frequency curve $d(f)=fft(h,-1)$. This curve is then multiplied by a Butterworth low pass filter array f which can be described as follows:

$$f(x) = \frac{1}{1 + \left(\frac{d(x)}{d_0}\right)^{2n}},$$

where n is the order of the filter and d_0 is the cutoff frequency. We used a value of $n=5$ (by experimentation) and $d_0=30$ as a compromise between an accurate approximation of the original shape and a reduced sensitivity to rapid changes in the histogram shape. This smoothing algorithm was found to provide generally accurate and robust fit to the original histogram curve, except for occasional problems near the endpoints of the histogram ($DN=0$ and $DN=255$). These did not create problems for the FHQ and could possibly be reduced by using another type of filter. The smoothed curve was employed in finding values for parameters in Eq.[1]-[3].

Given a specific histogram, the smoothed curve and its extreme points (two peaks and minima) were first computed and displayed using a specifically designed algorithm. It distinguishes the

second peak from smaller local peaks. The histogram segments containing the inflection points of interest were then identified by the analyst (e.g., the segment between the local minimum between the two peaks and the main peak, for the lower inflection point) and the program computed the exact inflection point locations.

2. Histogram Equalization algorithm (EQU). The underlying principle of the EQU is that each histogram level in the quantized image should contain an approximately equal number of pixels. First, the target number of pixels was computed by dividing the total number of image pixels (NP, excluding background such as image zero-fill) by TNL (the number of levels obtained by FHQ). EQU then begins adding pixels from the lower end of the histogram until the sum reaches NP/TNL, thus constituting the first quantized level n_1 . The second quantized level n_2 is determined as the first DN level greater than n_1 which exceeds the value $2*(NP/TNL)$; and so on. Note that sometimes two or more levels n_j will map to the same output value. In such cases the greatest n_j is chosen, thus the TNL for EQU may be less than for FHQ.

3. Normalization algorithm (NOR). This method involves the fitting of the histogram of the original image to a Gaussian distribution (Mather, 1987). First, the histogram range $\langle -3*stdev, 3*stdev \rangle$ is divided into TNL parts to obtain levels x_1, \dots, x_{TNL} . Then, for each segment $[x_i, x_{i+1}]$ the probability integral p_i is computed:

$$p_i = \int_{x_i}^{x_{i+1}} C e^{-ax^2} dx, \quad [5]$$

where C and a are constants. Then one computes

$$l_i = NP * p_i,$$

$$L_i = \sum_{k=1}^{k=i} l_k,$$

where l_i and L_i are the probabilistic number of pixels in quantized level i and the cumulative sum of the pixels for levels $\langle 1, \dots, i \rangle$, respectively. For each level i one then computes the actual cumulative number R_i as the sum of all histogram pixels for levels $\langle 1, \dots, i \rangle$:

$$R_i = \sum_{k=1}^{k=i} r_k,$$

where r_k is the number of pixels in the segment (k, k+1).

Starting with $i=1$, the lowest value k for which L_i exceeds some R_k is found. The the value i is mapped onto level k.

4. Linear Histogram Equalization method (LHQ). Given V_{max} (V_{min}) as the maximum (minimum) pixel value in the original histogram, the range $\langle V_{min}, V_{max} \rangle$ is divided into TNL levels of equal widths. The level in the original histogram S_n which corresponds to a quantized level n is computed as

$$S_n = V_{\min} + n \frac{V_{\max} - V_{\min}}{TNL}. \quad [6]$$

5. Linear Scaling (SCA). This algorithm performs a linear stretch of the original image to the image with output gray level $S(n)$ range from 1 to TNL according to the formula:

$$S_n = \frac{n(TNL - 1) + V_{\max} - TNL * V_{\min}}{V_{\max} - V_{\min}}, \quad [7]$$

where n is the number of individual DN values in the range $\langle V_{\min}, V_{\max} \rangle$.

Using each of the five above quantization algorithms, a new quantized image (QI) was produced in which the original digital value was replaced by the mean value for the quantized level; the mean was obtained by overlaying the quantized image onto the original image. A difference image (DI) was then computed for each algorithm on a pixel-by-pixel basis:

$$DI(i, j, k, l) = OI(i, j, k, l) - QI(i, j, k, l) + 128, \quad [8]$$

where DI, OI and QI are the digital values in the difference, original and quantized images, respectively; i is the image identification; j is the spectral band; k is the algorithm identifier, and l refers to pixel location. The constant was added to retain cases where $OI(i, j, k, l) < QI(i, j, k, l)$.

The average quantization error QE was then computed as

$$QE(i, j, k) = \frac{\sum |DI(i, j, k, l) - 128|}{NP}, \quad [9]$$

where the summation is made across all pixels NP in the image (excluding background). In addition, a normalized quantization error NQE was computed to compare the performance of the FHQ with the other algorithms, as:

$$NQE(i, j, k) = \frac{QE(i, j, k)}{QE(i, j, FHQ)}. \quad [10]$$

QE and NQE were computed separately for the entire histogram and for land pixels only. 'Land pixels' were defined for this purpose as those between the local minimum (separating the land and water peaks) and the gray level at which the cumulative histogram reached 97%. In other words, the last 3% of the pixels were not considered to be land. This was an arbitrary choice but

it does not significantly affect the analysis because the same value was used for all the algorithms. It is also used in image analysis software packages.

Results and discussion

Effectiveness of quantization algorithms

Figure 4 shows examples of the histograms used in testing the performance of the various quantization algorithms. These are narrow peak histograms, typical of red reflectance channels of vegetated land (Figure 4a); scenes with a significant portion of open water and closely (Figure 4b) or more widely (Figure 4c) spaced water and land peaks; scenes dominated by open water (Figure 4d); and scenes with wide histograms, typical of AVHRR data (Figure 4e). No images with more than two main peaks were found in the data set, as would be expected for growing-season images portraying terrestrial ecosystems. The distinctions among the above categories are important because of the desire to minimize the number of quantized levels while retaining the maximum possible information content of the original data.

Figure 5 shows the quantization errors QE produced by the various algorithms as the average difference between the original and the quantized pixel values. Their values ranged from <0.5 to >4.0 due to the different histogram shapes but several trends emerge. The overall trend was $FHQ \leq EQU < NOR < LHQ < SCA$. In general, FHQ yielded a lower quantization error than the other algorithms but the overall difference from the EQU was small. The LHQ and SCA errors were the largest overall. In case of the normalization method, most quantization errors were intermediate between those of FHQ/EQU and LHQ/SCA. In some extreme cases the NOR errors were quite small (e.g., 1327-3, Figure 4a) or very large (e.g., AVHRR-4, Figure 4e), depending on the extent to which the histogram could be accurately reproduced by a Gaussian distribution.

Figure 6 a shows the average quantization error QE of the various algorithms and histogram curves for all pixels in the scene. The average error was lowest for the FHQ and all curve types, except for histograms with one peak (two distant peaks) where the NOR (EQU) had somewhat lower quantization errors. The LHQ and SCA errors were systematically higher than those for the FHQ. Again, the normalization method showed variable results, best for single peak histograms but the worst for other histogram types. The overall mean quantization error (for all histogram groups, Figure 4) was 1.68 (FHQ), 1.79 (EQU), 2.17 (NOR), 2.18 (LHQ), and 2.33 (SCA). Considering land pixels only (Figure 6b), the results were qualitatively similar. The FHQ errors were still lower than for the other methods but comparable to EQU for three histogram groups. The difference between LHQ and SCA diminished further. The normalization error increased substantially compared to the other methods and showed clearly that because of its inconsistency, this algorithm is not suitable for the quantization for land mapping purposes. The

average QE decreased compared to the whole scene, with values 1.41 (FHQ), 1.51 (EQU), 2.24 (NOR), 2.24 (LHQ), and 2.28 (SCA).

Figure 7a compares the quantization errors of the various methods relative to that of the FHQ (Eq. 10). The FHQ produced a lower quantization error than the other algorithms in all cases except one, histograms with two distant peaks. This is where the EQU adjusts more readily to the increasing values because it responds only to the number of pixels while the FHQ also takes into consideration the width of the adjacent quantized level. Note, however, that the difference in relative error was small (0.04) while overall the NQE value for the FHQ was substantially lower than for the remaining combinations. Overall, the efficiency was 1.12 (in relation to EQU), 1.32 (NOR), 1.65 (LHQ), and 1.69 (SCA) when considering all scene pixels. While the trend remained unchanged for land pixels (Figure 7b), the NQE values increased substantially (to 1.65 for NOR, 2.40 for LHQ, and 2.48 for SCA) except for the EQU (1.11).

Comparison of flexible (FHQ) and equalized (EQU) quantization

The above results show that for a fixed number of quantized levels, the FHQ is substantially more efficient in retaining image information than the other quantization algorithms. Since the quantization error QE of the FHQ would also decrease with increasing DNL, these results can be considered generally valid for the types of histograms represented in the study. The EQU results, although still lower than those for the FHQ, indicate that the EQU is a good quantization algorithm for an overall scene representation. However, it is important to note that the low QE and NQE values are achieved by the EQU through finer quantization near the peaks of the histogram and coarser quantization in the histogram tails. This is illustrated in Figure 8a which shows the fraction of quantized levels inside the land histogram peak (as defined by the inflection points, ilp) as well as left (llp) and right (rlp) of the peak. The fraction of levels inside the land peak is higher for EQU than for FHQ, and the proportions of levels outside of this peak are correspondingly higher. The faster increase in QW of the EQU method outside the inflection points is shown in Figure 8b. Here, level #1 corresponds to the quantized level just inside the inflection point, level #2 contains the inflection point, and levels #3-5 are located outside the inflection point. Each histogram is represented by an average value for the two sides of the land peak and the value was computed as the QW for the EQU divided by that for the FHQ. Only histograms with 3 or more levels outside both inflection points for both methods are shown which represents 41% of the histograms in Figure 4. (In the remainder, 35% had <3 such levels at one or both sides of the land peak for both methods, and in 24% the FHQ had ≥ 3 levels (at both sides) but the EQU had <3 at one or both sides on the land peak.) Figure 8b shows that outside of the inflection points (positions #3, #4) the EQU levels were considerably wider than for the FHQ. This is also generally the situation for position #5, although in some cases the QW decreased, most often because the quantized levels contained part of a second histogram peak (water) and the QW for the FHQ decreased more gradually.

Comments

Results in Figure 5 through 8 show that the FHQ is an effective approach to image quantization for land cover mapping studies. Its performance is superior to three of the quantization algorithms tested: normalization, linear quantization, and scaling. While it also performed somewhat better than the EQU on the average, its main advantage with respect to the EQU is greater sensitivity to rare land cover types which may occur in the tails of the land peak. In the histograms examined, the number of levels decreased from 8 bits to <5 (14-30 quantized levels in most cases, average 23.3). These results are valid for various histogram shapes and for images consisting mostly of land and open water.

Although the approach was developed to minimize the loss of information on land cover, it could equally well be applied to other elements of the scene, e.g. to optimize the representation of open water bodies. It has not been tested for scenes consisting of multiple peak-histograms where all elements are of equal interest. Such examples were not encountered in among the growing-season TM and AVHRR data. It should also be noted that while the FHQ result is produced automatically, the analyst can intervene in the selection of the peaks of interest. For example, the analyst may wish to give equal emphasis to land and water peaks, and thus choose the appropriate inflection points. The possibility of intervention also gives the analyst an opportunity to evaluate the correctness of the identification of the histogram maxima and minima; and to deal with unusual cases, such as three-peak histograms.

FHQ has been designed to reduce the number of levels as much as possible, thus increasing the speed of computer classification procedures such as the Classification by Progressive Generalization (Cihlar et al., 1998). As computer speed increases, a higher number of quantized levels can be employed without slowing down the computation process. This can be easily done by increasing the value of a (Eq. [1]), without the need for further tests and adjustment. Note that because of Eq. [3] the overall number of levels will increase by more than the increase in a .

Since values of $f < 0.5$ (Eq.[1]) were not encountered in this study we could not evaluate the impact of Eq.[1b]. By definition, it is very unlikely that low values of f will be found in an image. Nevertheless, such instances could be readily accommodated by making $c \gg d$ in Eq. [3].

A qualitative comparison of the original and quantized images showed that for boreal ecosystem images, FHQ results in a minimal loss of land cover type information. When displayed as a colour combination of three channels the difference between the original and the quantized images can be visually discerned only after a significant enlargement (factor of 16 or more) and only in some cases; even then, the pattern is mostly preserved but the colours of the pixels change somewhat. Indeed, in many cases it is very difficult to visually distinguish the

original from the quantized image. It is therefore not clear how much of the spectral variability within-cover types has been lost by the FHQ process. However, there has been a substantial reduction in the data complexity. Starting with a theoretical maximum of 1.68×10^6 possible spectral combinations for the three-band image the number has been reduced to about 1.26×10^4 (23.3×3), or a factor of approximately 1300. Based on the findings with the data sets used the reduction is 10.94^n , where n is the number of spectral bands used.

FHQ is designed to provide an optimal quantization of the data represented in the histogram of the image and the results are thus sensitive to the scene content. This makes the preservation of scene information possible but has the disadvantage that the classification results will be scene-dependent. In the operator-controlled method used by Beaubien (1994) such dependence is reduced by identifying the same cover types as endpoints of the quantized image. In general, the dependence cannot be entirely eliminated because of atmospheric or phenological effects. With respect to mapping of adjacent scenes, the FHQ can be used in three ways. First, if the scenes can be adjusted to produce a radiometrically seamless product the FHQ can be applied after mosaicking in the same manner as for a single scene. Second, if only corresponding cover types can be identified (Beaubien, 1994) the FHQ can be used as formulated here but the inflection points replaced by digital values for the reference cover types (and the value of a in Eq. [1] increased by a safe margin). Third, if none of the above are possible, the value of a can be increased as much as feasible so that many spectral clusters are produced; the among-scene differences can then be reconciled through the labeling process.

Conclusions

In this study, we have devised and tested an algorithm which automatically and reproducibly quantizes an image into a reduced number of levels, without perceptibly reducing the land cover type-related information in the image. The Flexible Histogram Quantization (FHQ) algorithm is intended to provide an adequate quantization in the main histogram peak as well as in the tails of this peak. It assumes that the histogram has at most two main peaks (such as land and water) and that most of the information of interest is in one peak. The algorithm then computes the number of quantized levels and identifies the digital values belonging to each level.

A comparison of the FHQ with four other quantization algorithms showed that the FHQ retained substantially more information than histogram normalization, linear quantization, and scaling methods. Using a sample of Landsat TM images and an AVHRR coverage of Canada, the following results have been obtained:

1. Overall, the normalization, linear quantization and scaling algorithms were found inferior to FHQ and EQU in terms of quantization errors and consistency for various histogram shapes.

2. Overall, the flexible histogram quantization (FHQ) yielded somewhat lower quantization errors than histogram equalization. However, it showed much higher sensitivity to infrequent cover types, represented by the tails of the main histogram peak. FHQ also does not require prior knowledge of the number of quantized levels desired and can be implemented in an automated mode.
3. When comparing visually the original and FHQ-quantized images, the information loss could be discerned only at a large magnification and only in some cases, demonstrating that most of the land cover information was retained. Yet, the average data volume reduction was a factor of 10.94^n (about 1300 for a three band data set, $n=3$).

It is concluded that the FHQ is an effective pre-processing algorithm for land cover mapping applications of satellite multispectral data.

References

Beaubien, J. 1994. Landsat TM satellite images of forests: from enhancement to classification. *Canadian Journal of Remote Sensing* 20: 17-26.

Beaubien, J., J. Cihlar, Q. Xiao, J. Chen, K. Fung, and P. Hurlburt. 1997. A new, nationally consistent, satellite-derived land cover of Canada: a comparison of two methodologies. *Proceedings of the International Symposium "Geomatics in the Era of Radarsat, May 25-30, Ottawa, Ontario (published on CRROM)*.

Brigham, E.O. 1974. *The Fast Fourier Transform*. Prentice-Hall, Englewood Cliffs, NJ.

Cihlar, J., Xiao, Q., Chen, J., Beaubien, and Latifovic, R., 1998. Classification by Progressive Generalization: a new automated image analysis methodology for remote sensing data. *International Journal of Remote Sensing* 19: 2685-2704.

Cihlar, J., Beaubien, J., Xiao, Q., Chen, J., and Li, Z. 1997. Land cover of the BOREAS Region from AVHRR and Landsat data. *Canadian Journal for Remote Sensing* 23(2): 163-175.

Jensen, J.R. 1996. *Introductory digital image processing: a remote sensing perspective*. Prentice Hall, Upper Saddle River, New Jersey. 316p.

Mather, P.M. 1987. *Computer processing of remotely-sensed images*. John Wiley & Sons, Toronto. 352p.

PCI. 1997. *EASI/PACE Image Processing Kit, version 6.2*. PCI Inc., Richmond Hill, Ontario.
PVWAVE. 1993. *PV-WAVE Advantage. Programmer's Guide*. Visual Numerics, Houston, Texas. 498p.+App.

Rabben, E.L. 1960. Fundamentals of photo interpretation. In: Colwell, R.N. (Ed.), *Manual of photographic interpretation*, The American Society of Photogrammetry, Washington, D.C.: 99-168.

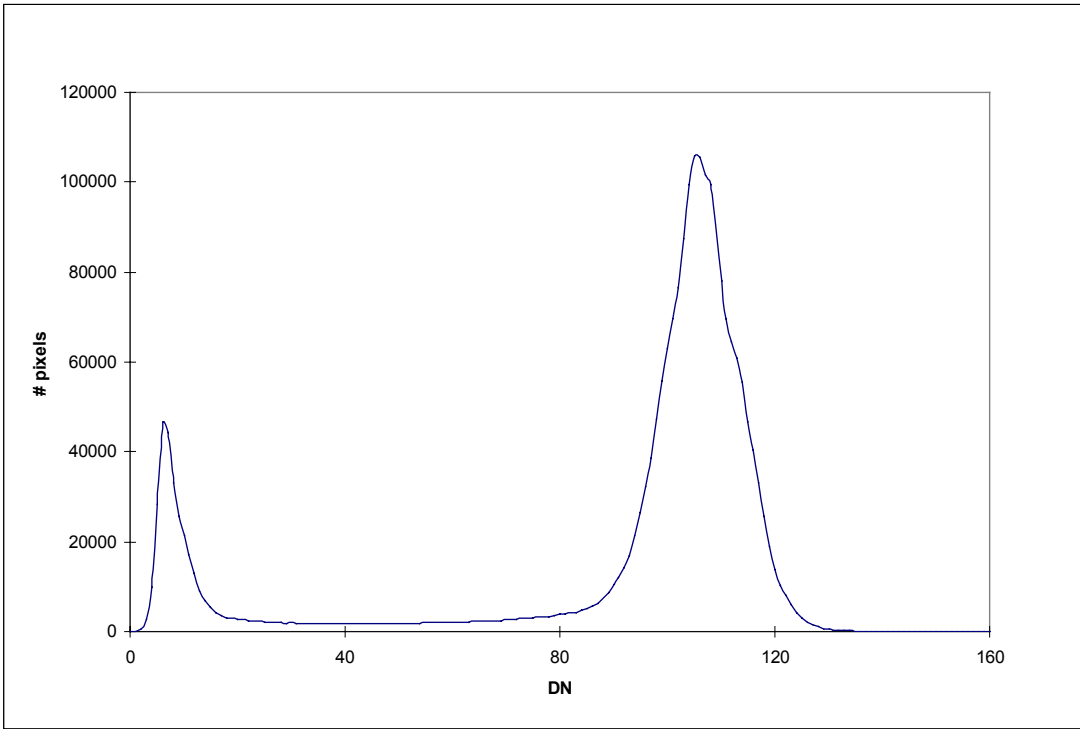


Figure 1. Histogram showing three regions with different characteristics from the viewpoint of quantization.

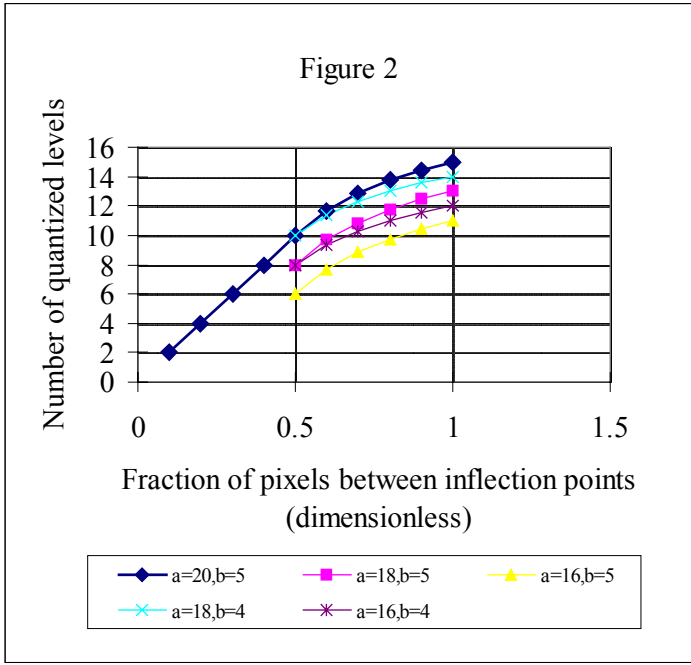


Figure 2. Computing the number of levels for the main

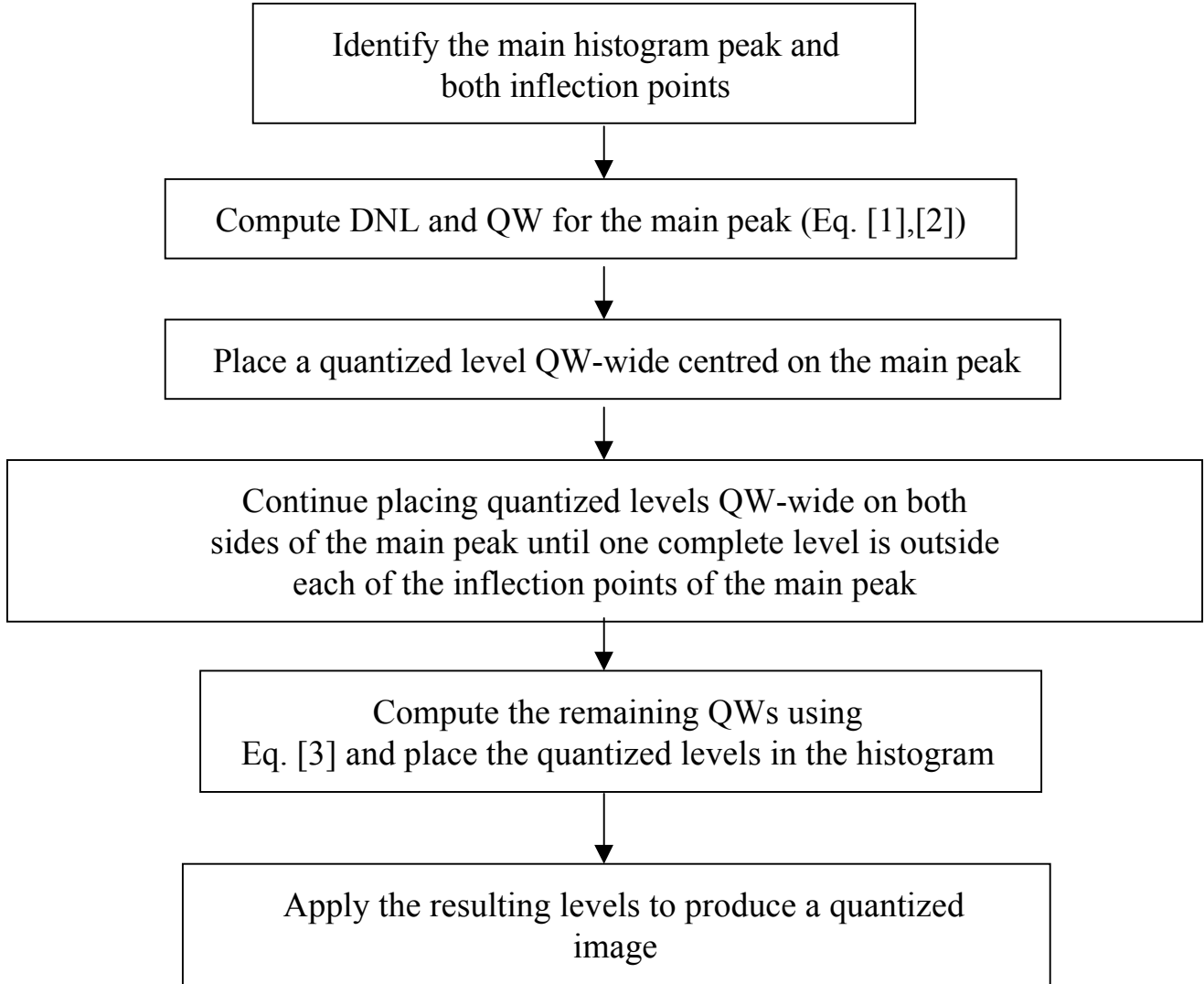


Figure 3. Flowchart for the Flexible Histogram Quantization algorithm.

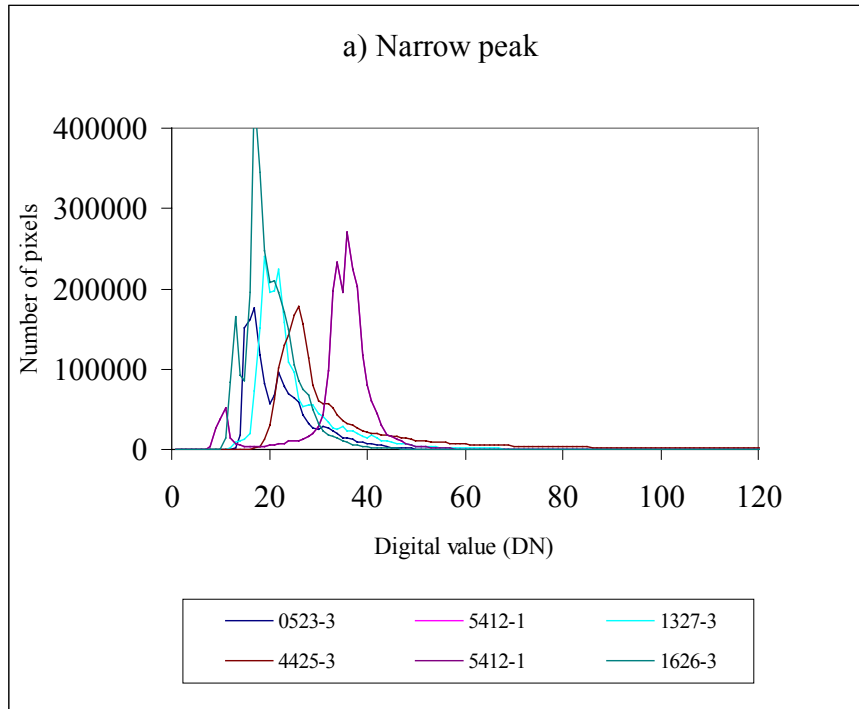


Figure 4a

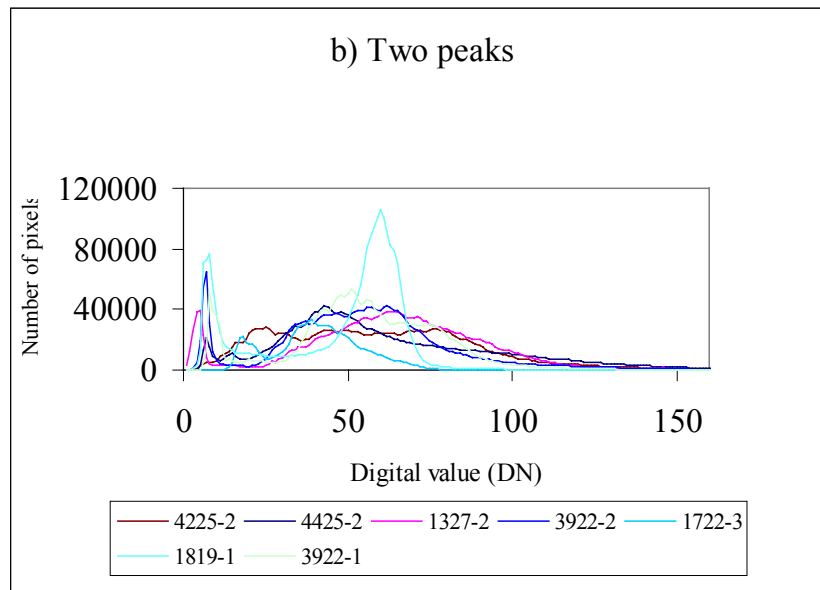


Figure 4b

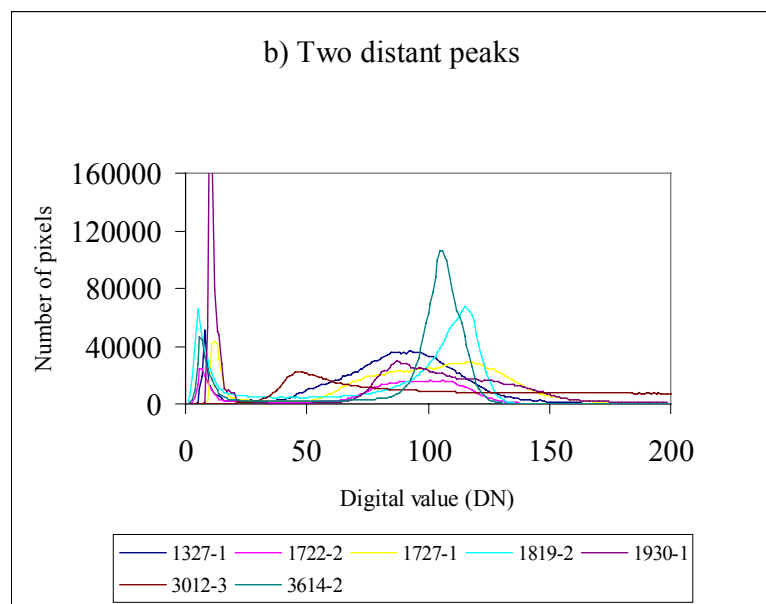


Figure 4c

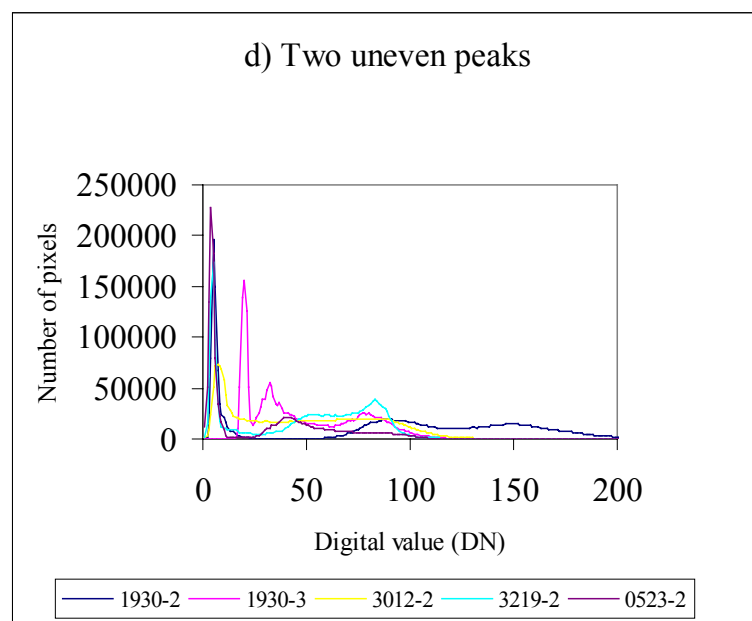


Figure 4d

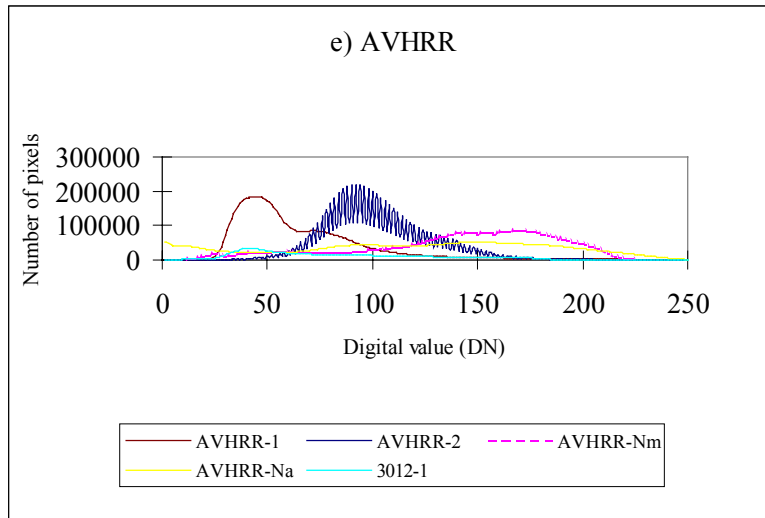


Figure 4e

Figure 4. Histograms used in the tests of the quantization algorithms. The histogram labels are $xyy-z$, where x = path, y = row, and z = TM band reference (1=band 4, 2=band 5, 3=band 3).

Figure 5

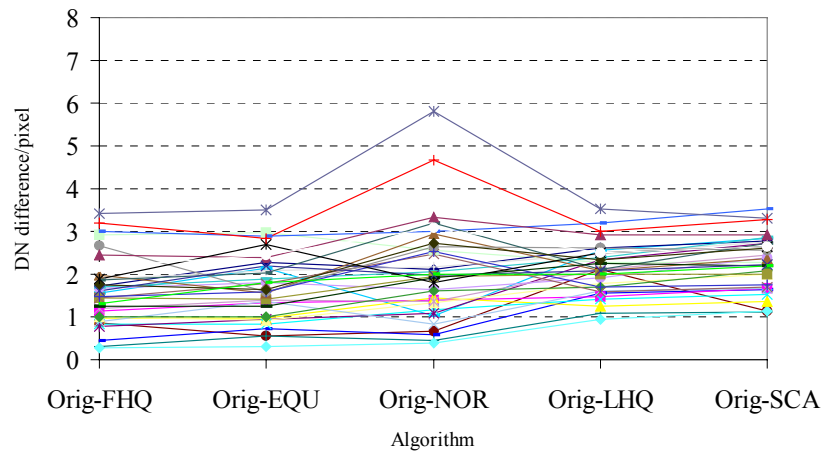


Figure 5. The average quantization error QE for various algorithms and images.

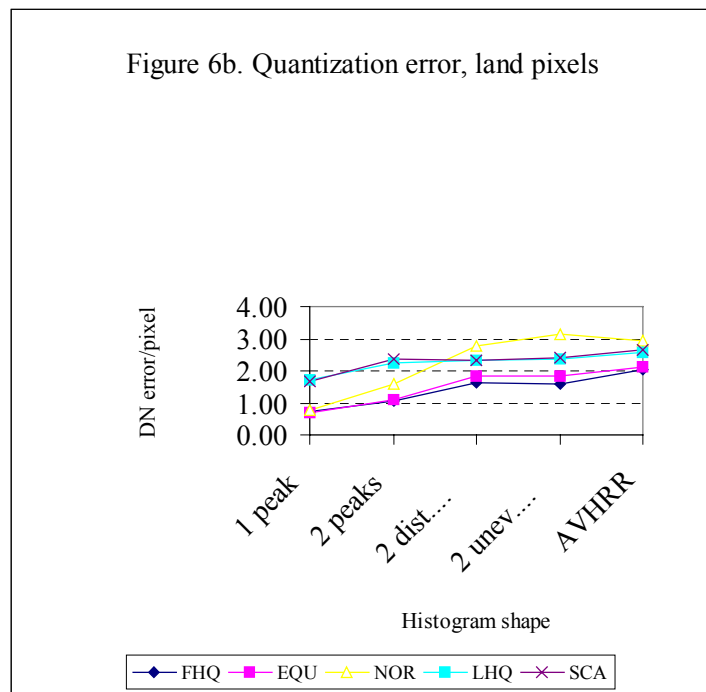
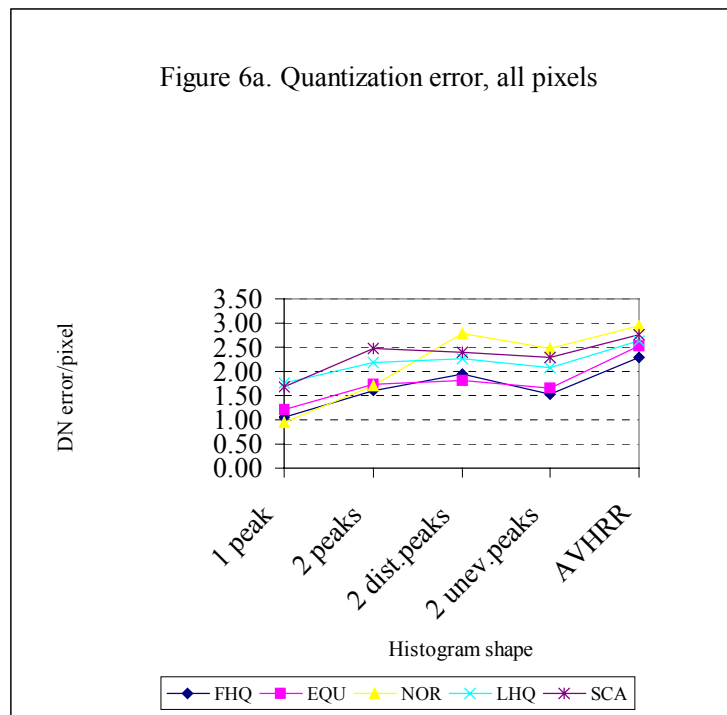


Figure 6. The average quantization error QE for various quantization algorithms and histogram shapes. Figure 6a: all image pixels. Figure 6b: land pixels only.

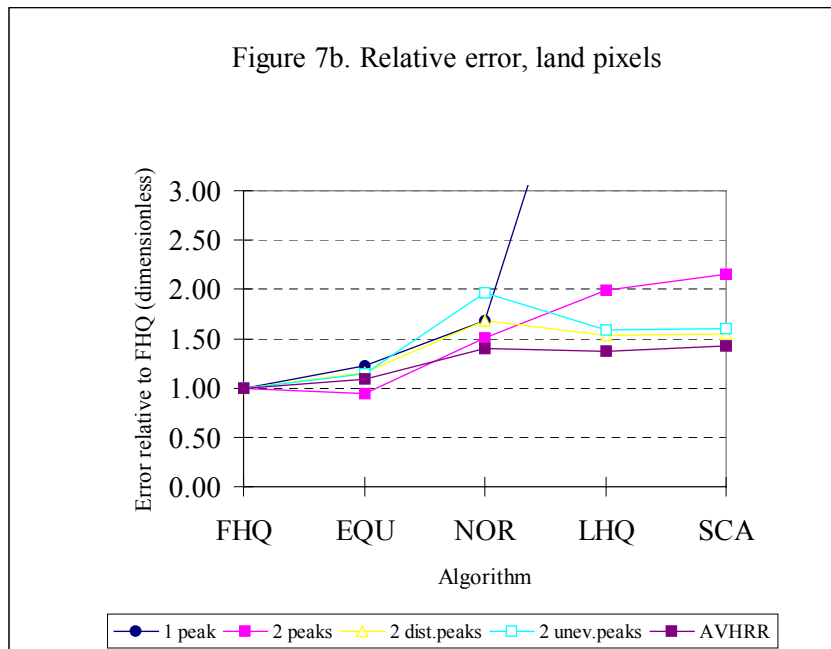
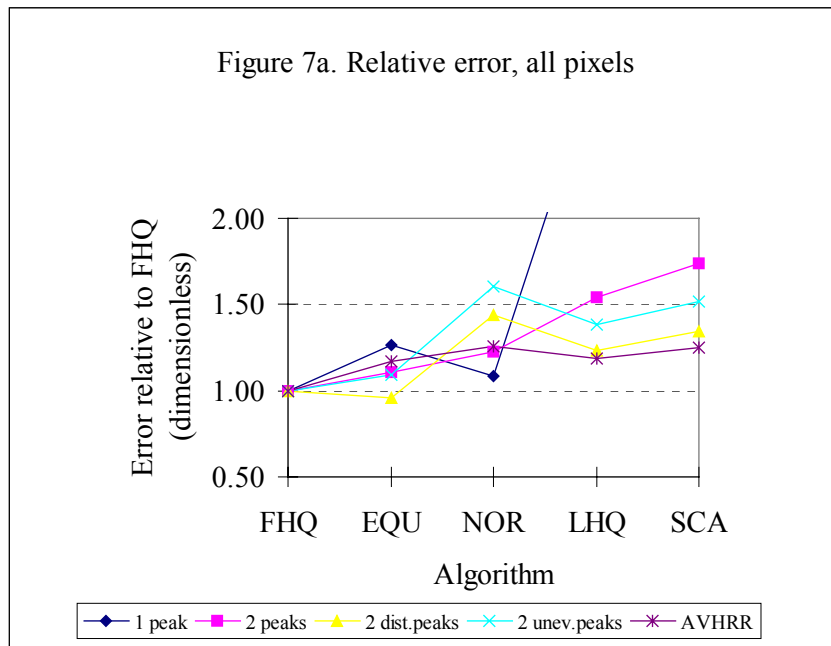


Figure 7. The relative quantization error for various algorithms and histogram shapes, in comparison to the flexible histogram quantization algorithm. Figure 7a: all image pixels. Figure 7b: land pixels only.

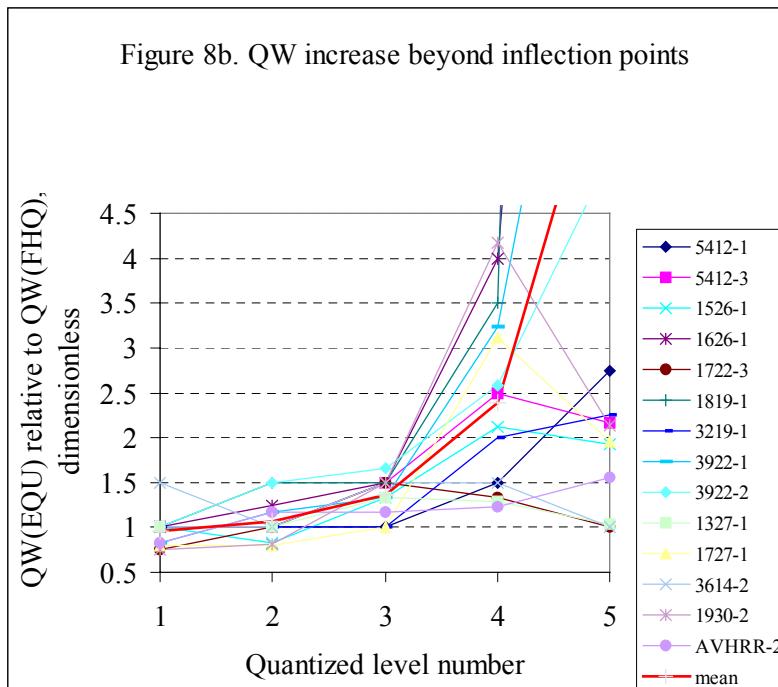
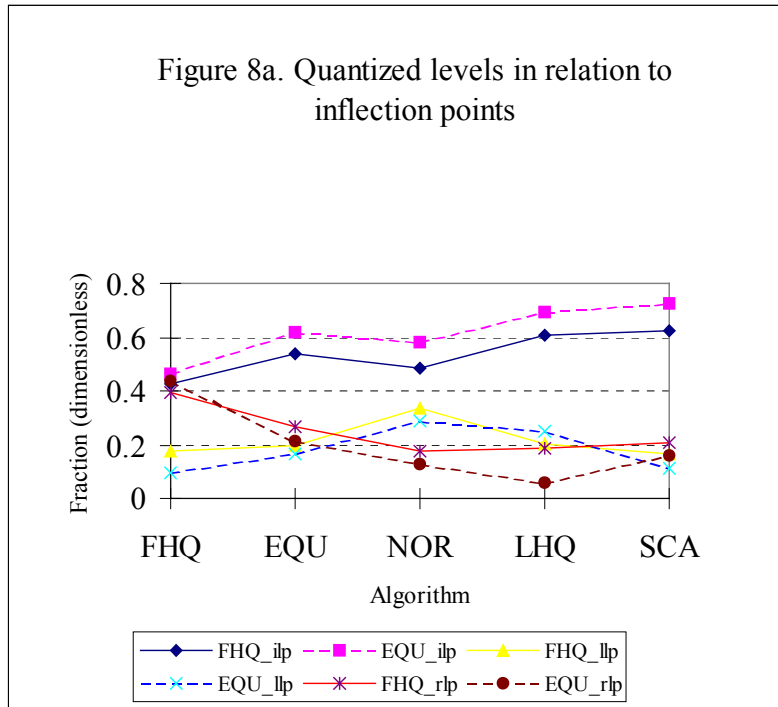


Figure 8. Comparison of histogram equalization (EQU) and flexible histogram quantization (FHQ). Figure 8a: The fractions of all levels inside (ilp), left of (llp) and right of (rlp) the main histogram peak. Figure 8b: The relative width of the quantized levels in the tails of the histogram (width of EQU divided by the width for FHQ).